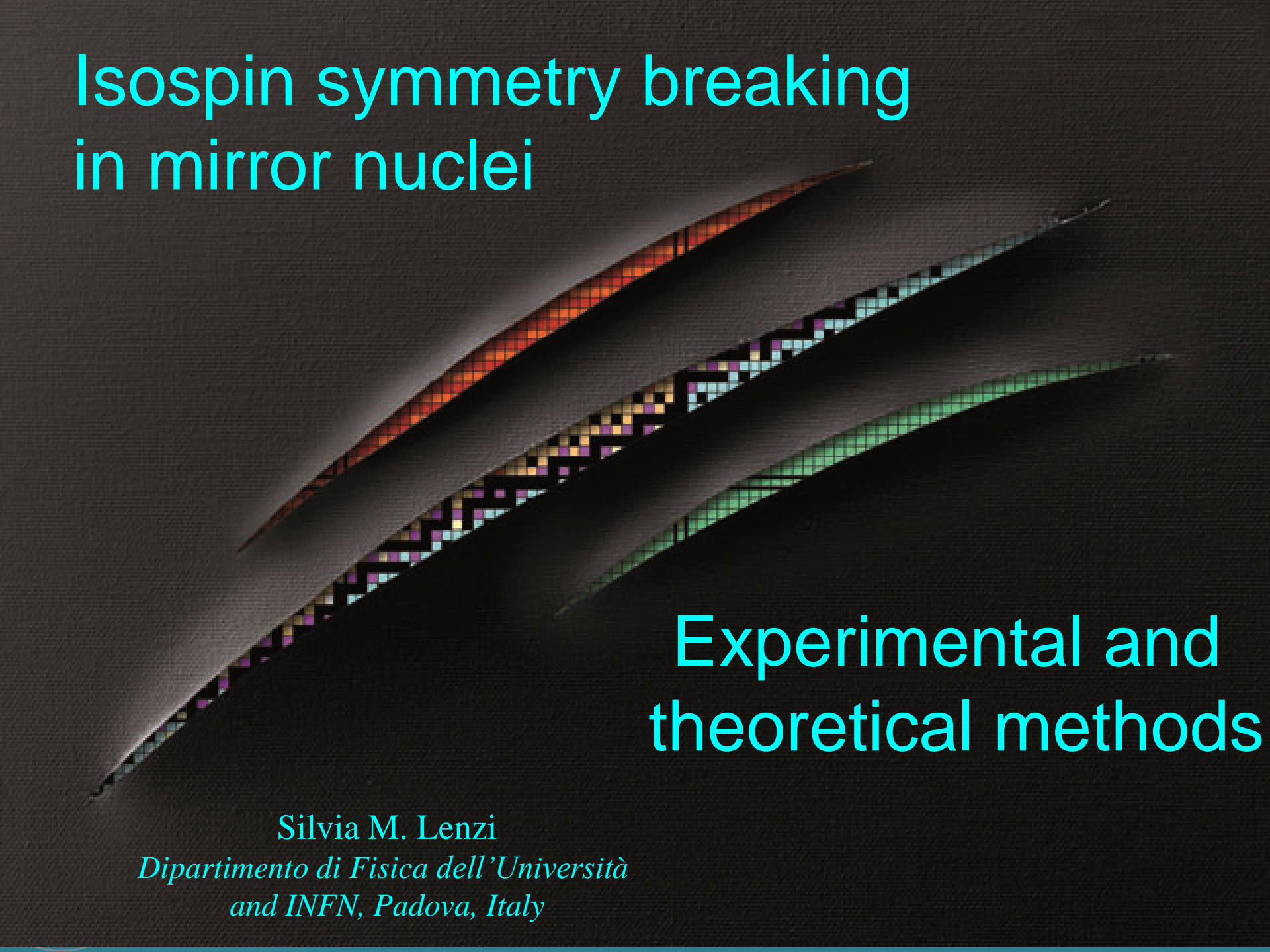


Isospin symmetry breaking in mirror nuclei

A graphic element consisting of a dark grey or black rectangular area with a diagonal tear starting from the top-left corner. The tear reveals a vibrant, abstract pattern of small colored squares (red, orange, yellow, green, blue) arranged in a grid-like fashion, suggesting a digital or microscopic image.

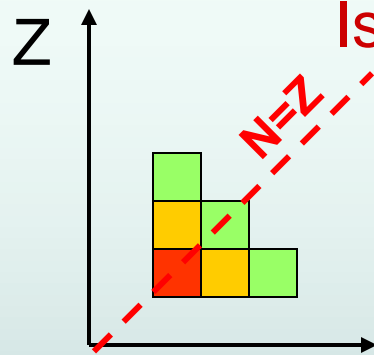
Experimental and theoretical methods

Silvia M. Lenzi

*Dipartimento di Fisica dell'Università
and INFN, Padova, Italy*

2. Experimental techniques for mirror spectroscopy

Coulomb Energy Differences (CED)



Isospin symmetry manifests better along the $N=Z$ line

Analogue states with low spin are studied in CDE (IMME)

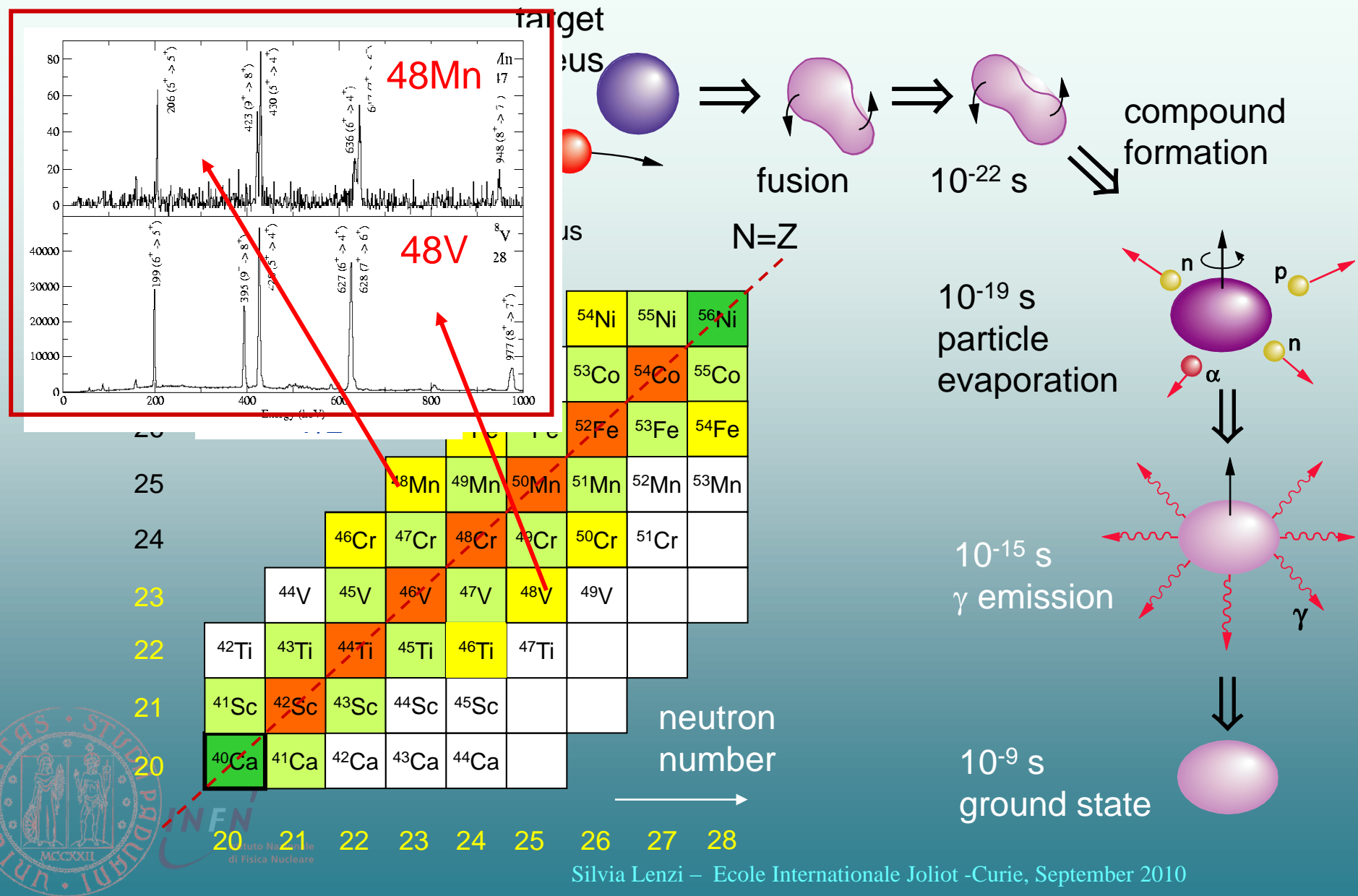
What about the difference in excitation energy with increasing spin?

CED have been restricted for many years to low-spin states due to the difficulties in populating proton rich nuclei...

Experimental issues

- proton-rich $T_z < 0$ isobars only weakly populated
- “mirrored” gamma-ray energies almost identical
→ we need very clean reaction channel selection...

Populating proton-rich nuclei

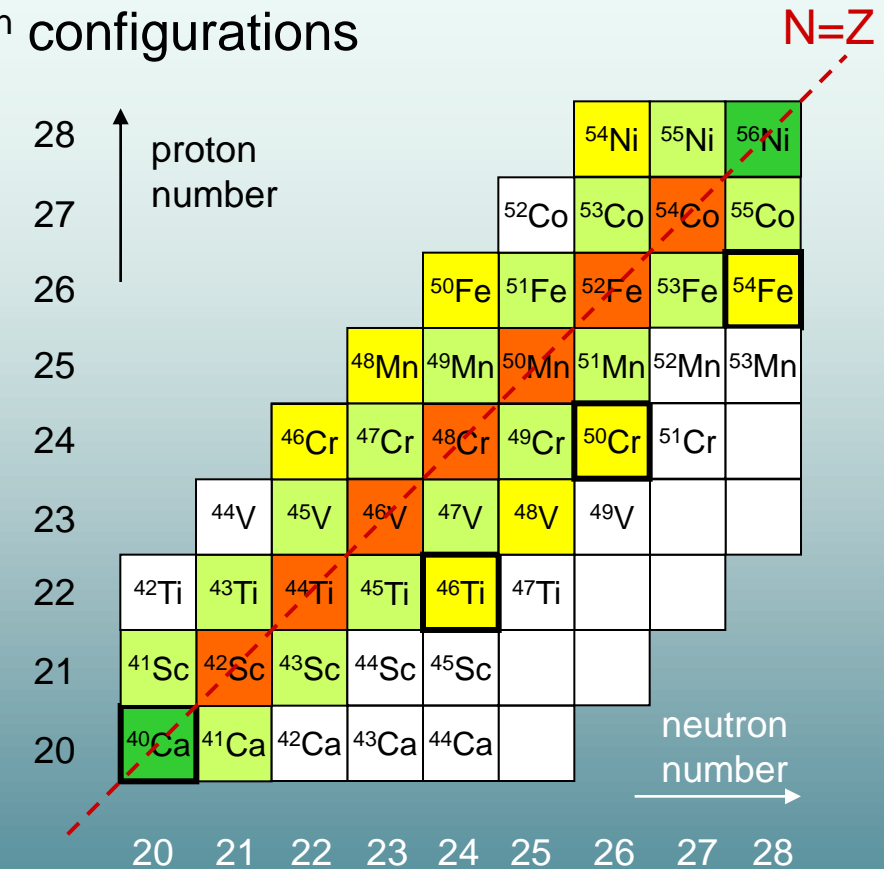
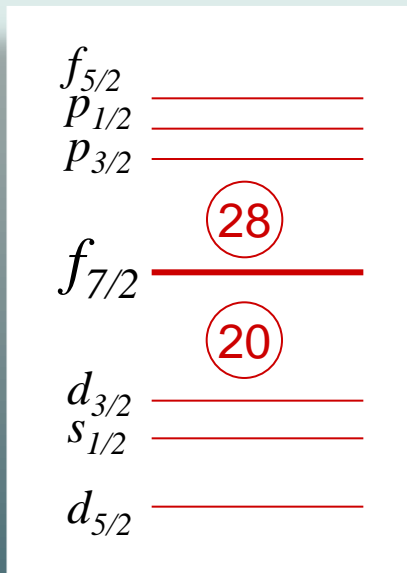


Example: the $f_{7/2}$ shell

The $1f_{7/2}$ shell is isolated in energy from the rest of fp orbitals

Wave functions are dominated by $(1f_{7/2})^n$ configurations

High-spin states experimentally reachable



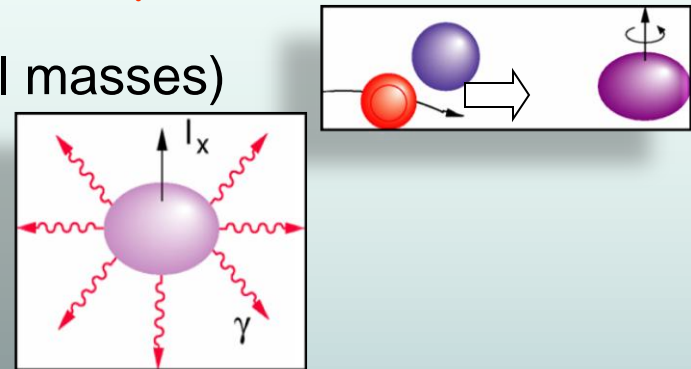
Experimental issue : proton-rich $T_z=-1/2$ isobars are weakly populated

“Mirrored” gamma ray energies almost identical – need very clean reaction channel selection...

Experimental requirements

High efficiency and resolution for γ detection

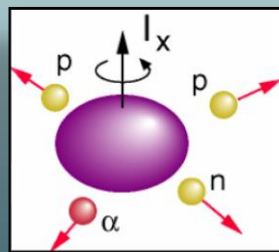
Low cross section at high spin (small masses)



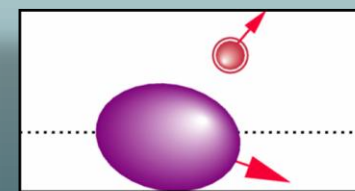
High energy transitions

Good selectivity: particle detectors

Many channels opened: high efficient charged-particle detectors



Kinematics reconstruction
for Doppler broadening



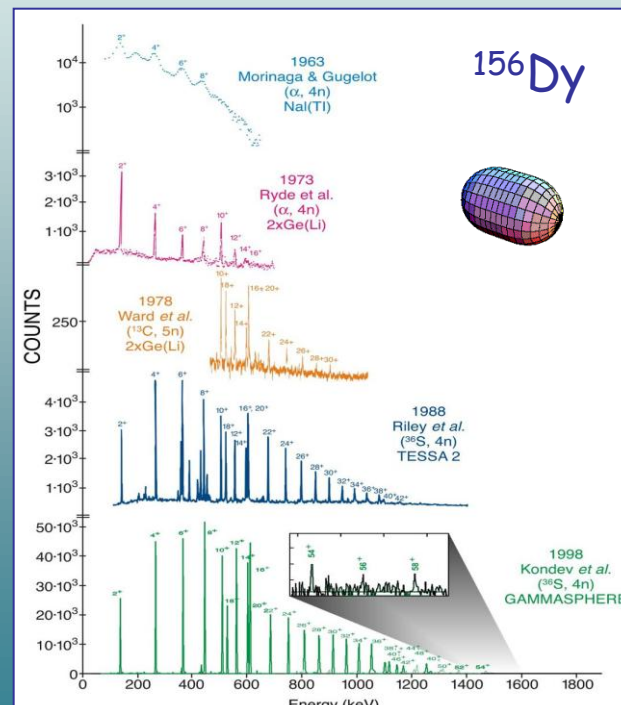
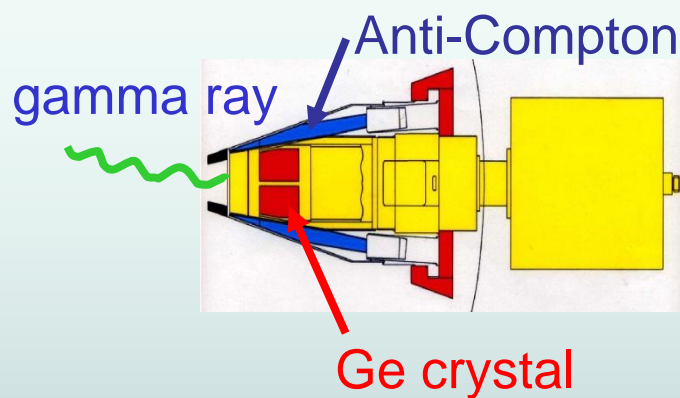
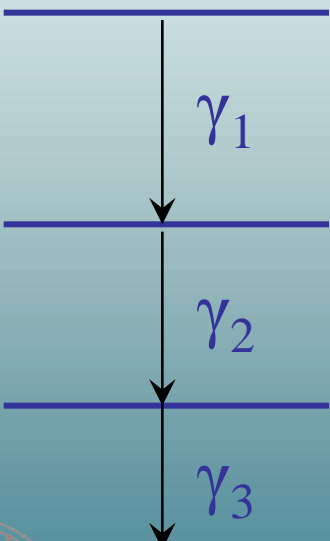
Mass spectrometers

Neutron detectors to select proton-rich channels

Polarimeters and granularity (J , π , δ)

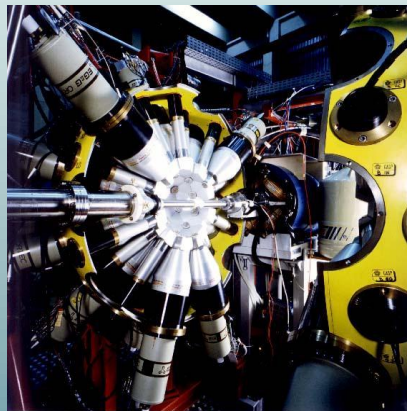
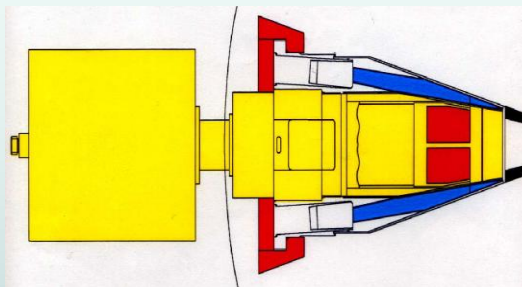
Gamma spectroscopy

Constructing
a level scheme



Gamma-ray spectrometers

Conventional techniques

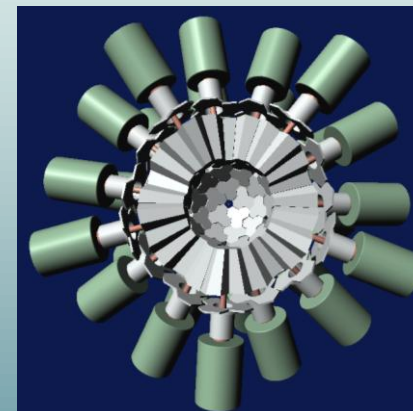
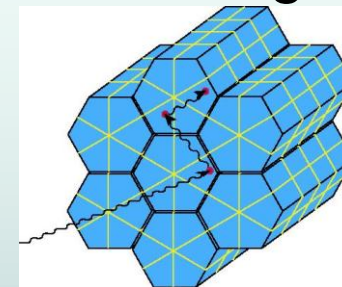


GASP

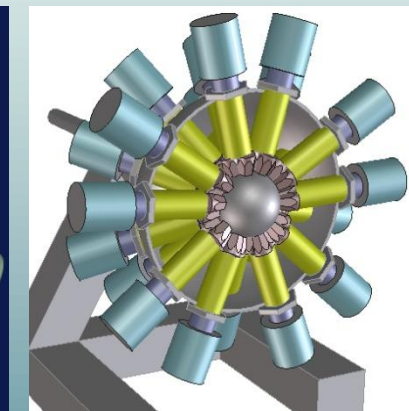


GAMMASPHERE

New technique:
tracking



AGATA

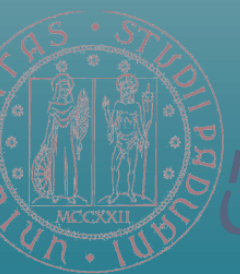


GRETA

$$\epsilon \sim 10 - 5 \% \quad (M_\gamma = 1 - M_\gamma = 30)$$



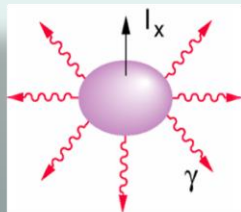
$$\epsilon \sim 40 - 20 \% \quad (M_\gamma = 1 - M_\gamma = 30)$$



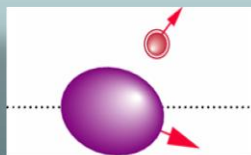
Istituto Nazionale
di Fisica Nucleare

Techniques for proton-rich spectroscopy

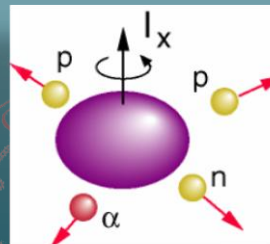
Three basic techniques for selecting proton-rich systems



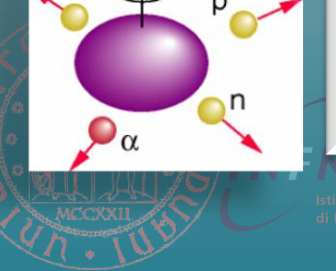
1. High efficiency & high granularity **gamma-ray spectrometer**
high fold γ^n ($n \geq 3$) coincidence spectroscopy



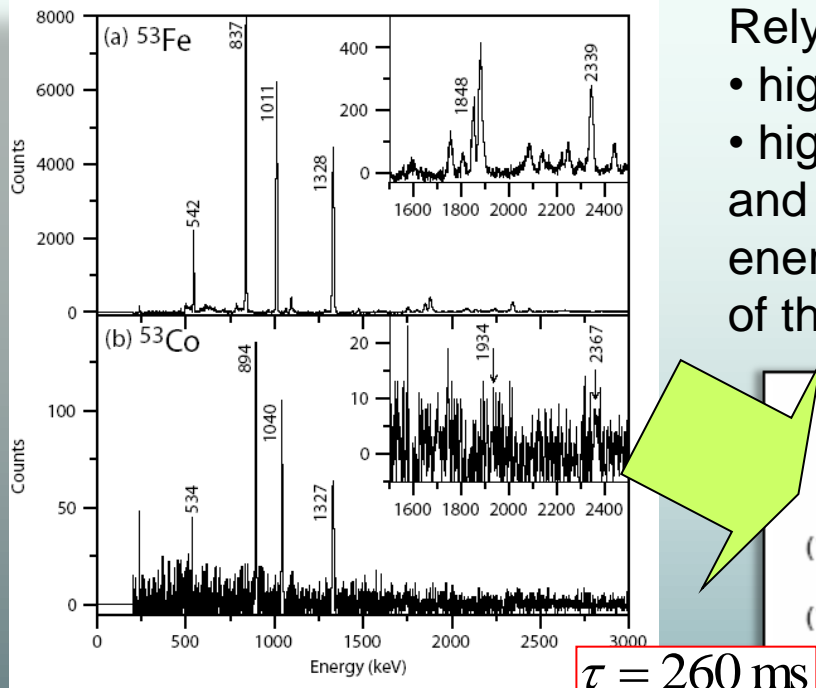
2. **Gamma-ray array + mass spectrometer + focal plane detectors** - identify A,Z of recoiling nucleus and ToF
→ tag emitted gamma-rays



3. Identify cleanly all emitted particles from reaction - needs a **charged-particle detector array + high-efficiency & high granularity neutron detector array + γ -ray array**



1. High-fold γ -coincidence spectroscopy



$\tau = 260 \text{ ms}$

Double-coincidence spectra after
gating on 2 analogue transitions

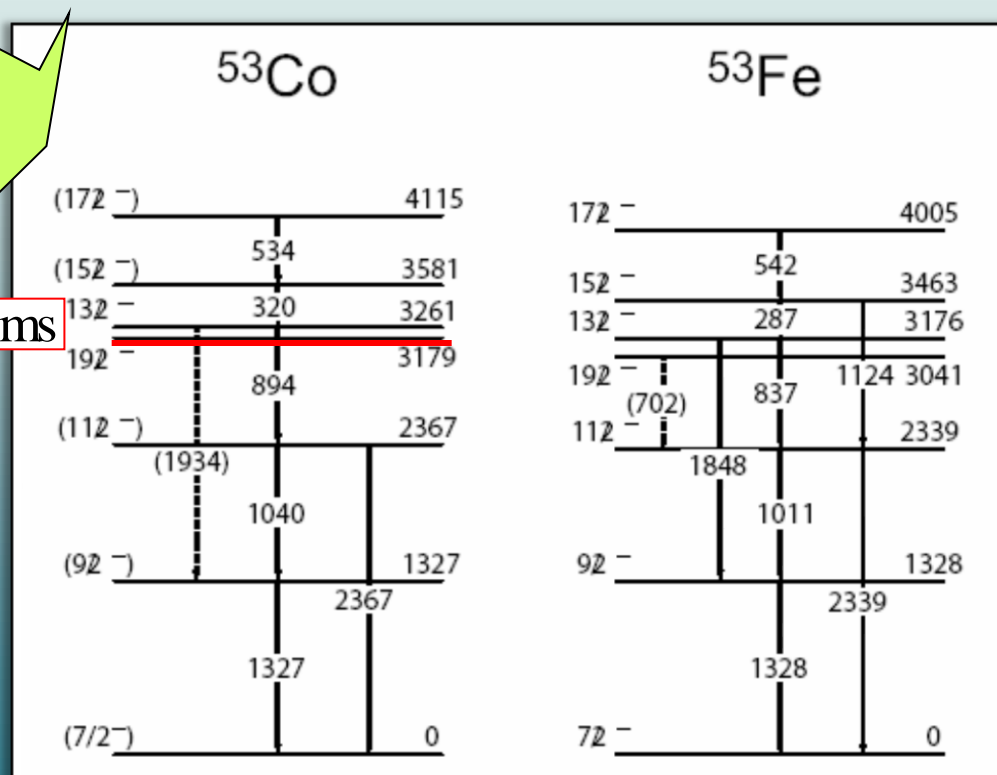
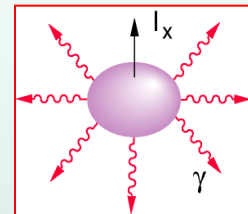


S.J. Williams et al., Phys. Rev. C 68 (2003) 011301

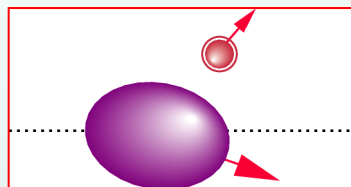
Rely on the power of the array:

- high-fold gamma ray coincidences
- high granularity...

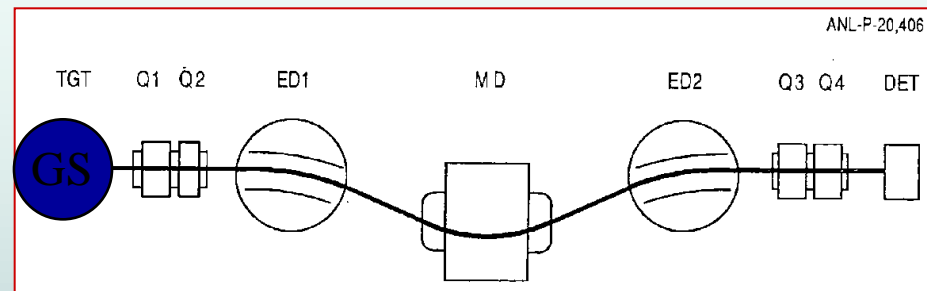
and on the similarity between the
energy of the transitions with those
of the known mirror nucleus



2. Identify A and Z of the recoiling nucleus



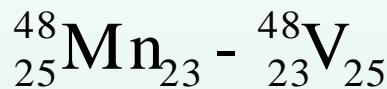
Fragment Mass Analyser



- Combined electric and magnetic dipoles → beam rejection & A/q separation
- A/q identified by x -position at focal plane
- Z identified by energy loss ($E-\Delta E$) in gas-filled ionisation chamber
- information used to “tag” coincident gamma-rays at target position
- Efficiency - up to $\sim 15\%$
- Measure the final residue



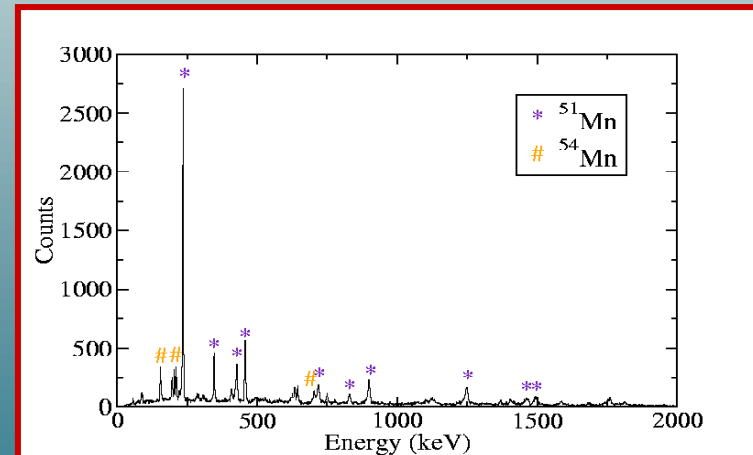
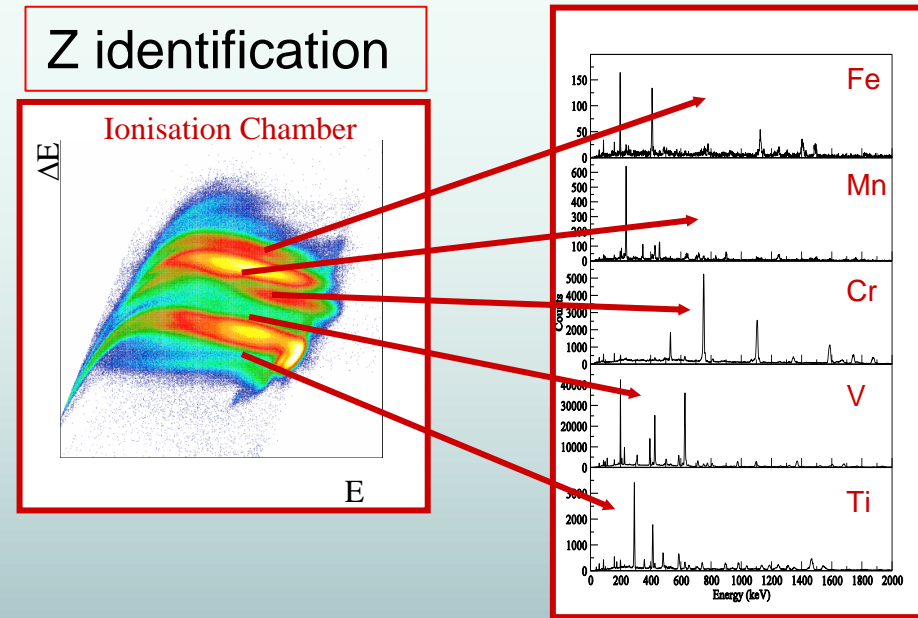
An example: the A=48 mirror pair



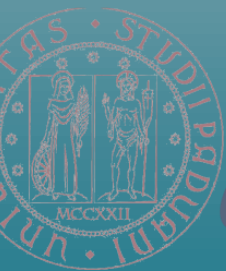
$$\frac{\sigma(^{48}\text{Mn})}{\sigma(^{48}\text{V})} \sim 10^{-4}$$

Need very good selectivity

A/q selection
at the focal plane
+
gate on Z=25



M.A. Bentley et al.,
Phys. Rev. Lett. 93 (2006) 132501



INFN

Istituto Nazionale
di Fisica Nucleare

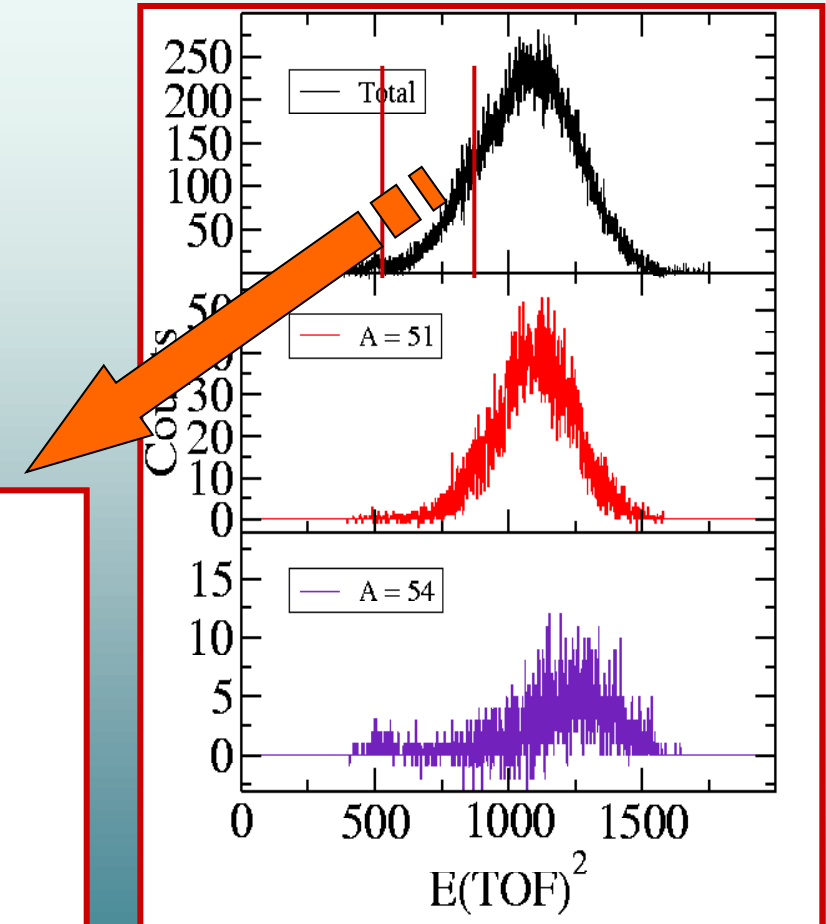
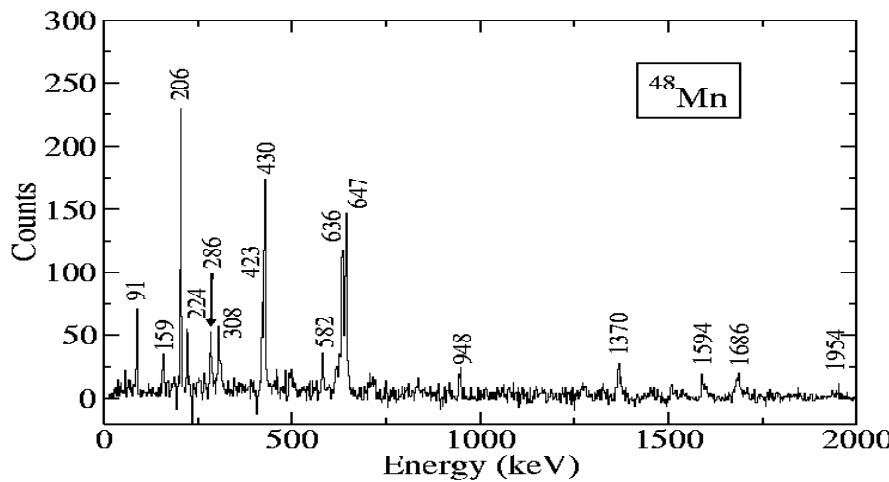
Selecting “pure” spectra

Contaminants can be removed by using the recorded total energy E and time-of-flight (TOF) of the recoils

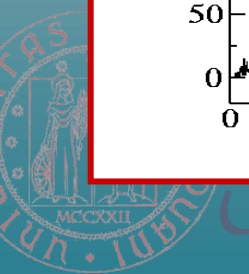
Mass is proportional to ET^2

$$E = \frac{1}{2}mv^2, \quad v = \frac{d}{TOF}$$
$$\Rightarrow m \propto E(TOF)^2$$

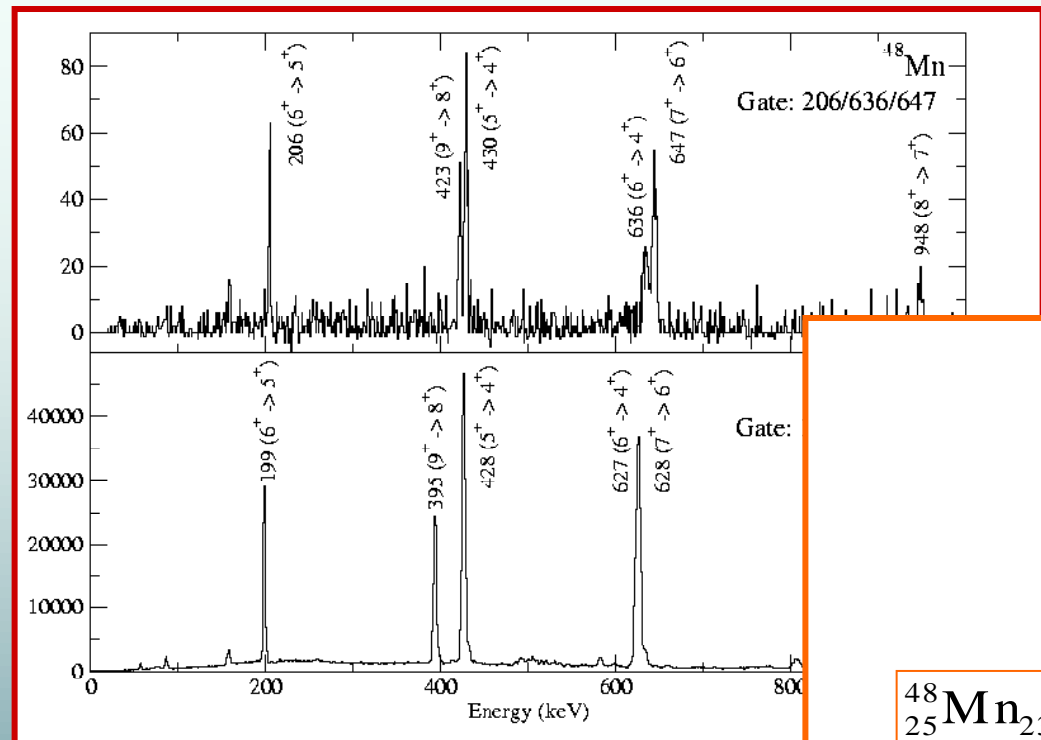
the ET^2 information has sufficient resolution to distinguish three mass units difference.



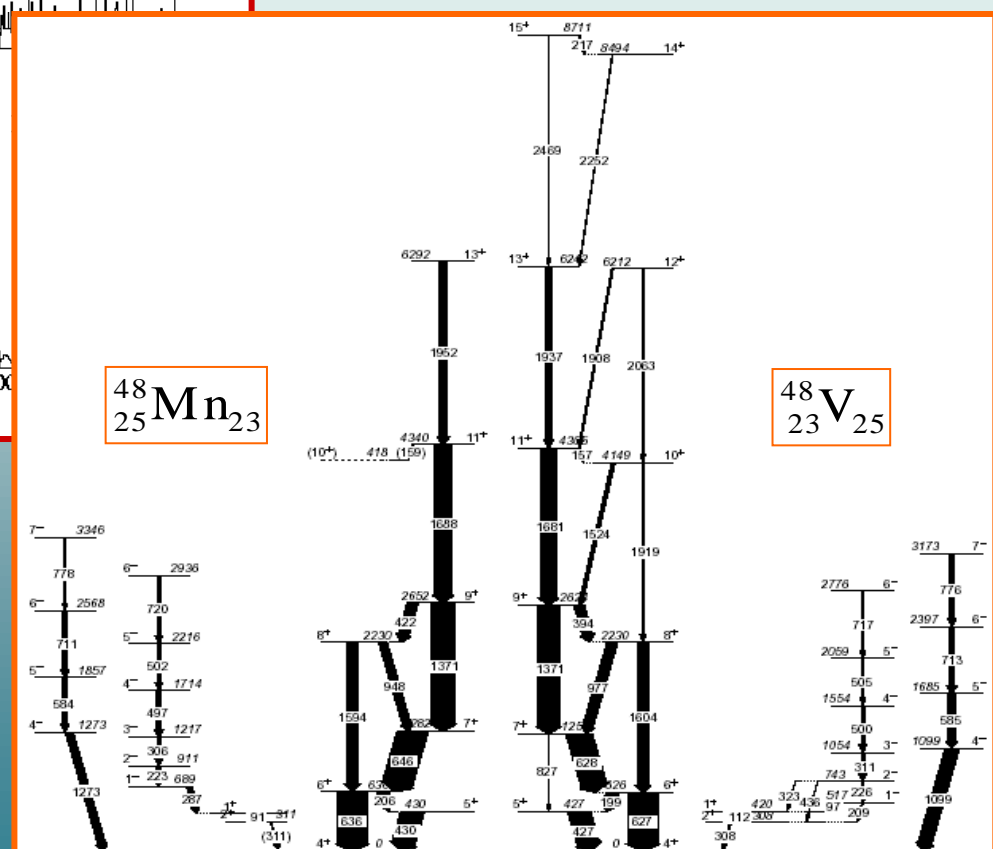
M.A. Bentley et al.,
Phys. Rev. Lett. 93 (2006) 132501



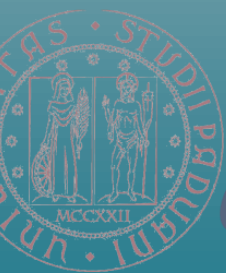
γ - γ coincidence analysis



(A/q = 3, Z=25)-gated and
E(ToF)²-gated
 γ - γ coincidence analysis...



M.A. Bentley et al.,
Phys. Rev. Lett., 97 (2006) 132501



INFN

Istituto Nazionale
di Fisica Nucleare

Fragmentation reactions and exotic beams

Fragmentation reactions with the removal of 5 or more particles are mainly of statistical character and populate yrast states.

One knock-out reactions are a direct process.

Two–proton knockout from neutron-rich nuclei and two–neutron knockout from proton-rich nuclei at intermediate or relativistic bombarding energies are also direct reactions.

Direct reactions selectively populate single-hole states

Between 3 and 5 nucleons removed the two processes compete

Fragmentation reactions are particularly suitable to populate mirror nuclei far from stability and near the proton dripline.

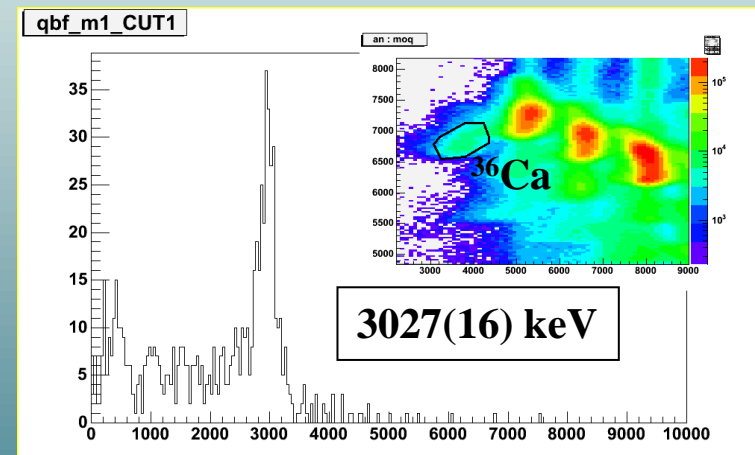
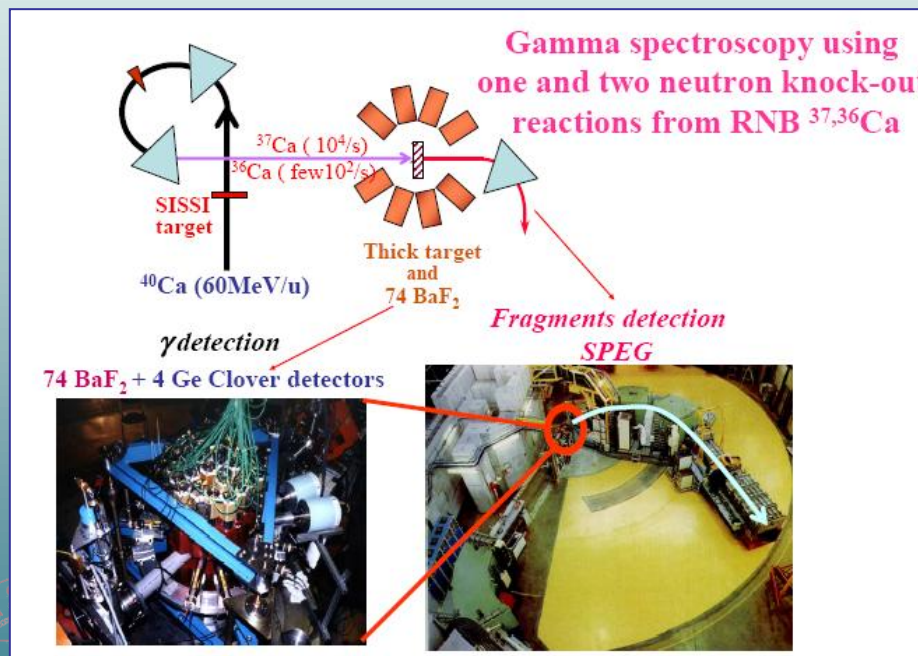


Knockout reactions with exotic beams

Example: study the “magicity” of ^{36}Ca – mirror of magic ^{36}S ($N=20$, $Z=16$)

One neutron removal reaction from ^{37}Ca beam

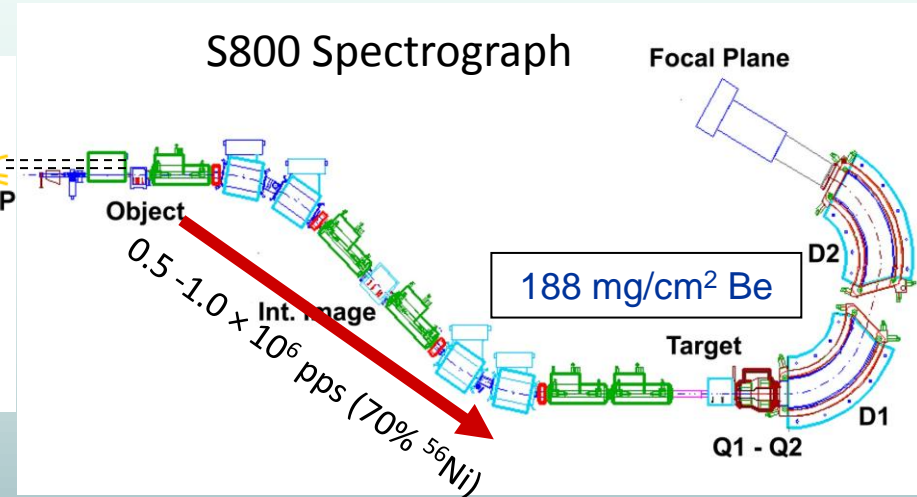
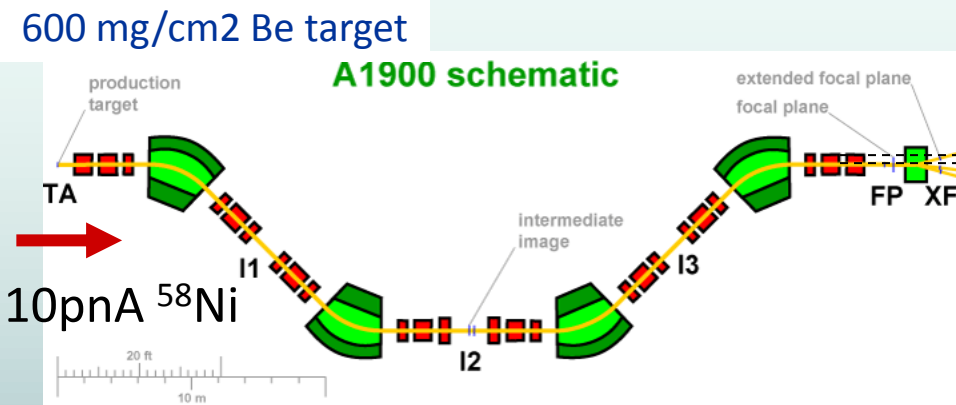
Technique pioneered at GANIL (Stanoiu et al. PRC 69, 034312 (2004))



F. Azaiez et al.

Mirrored fragmentation of N=Z nuclei

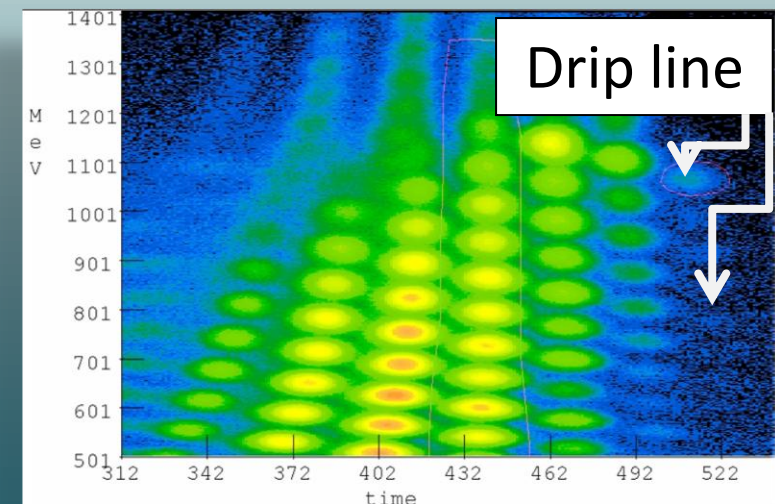
MSU experiment



Primary → N=Z second. → “mirrored frag.”

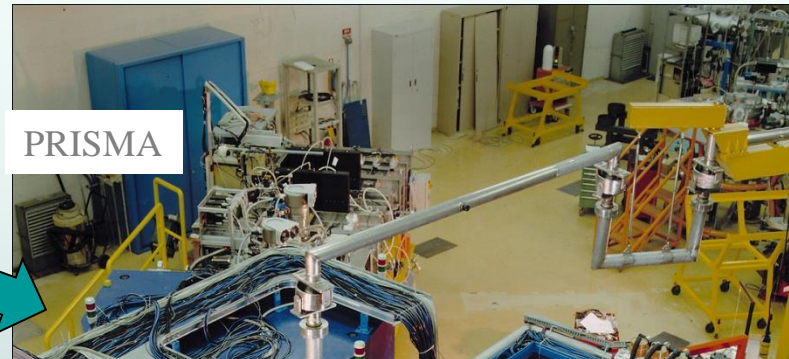
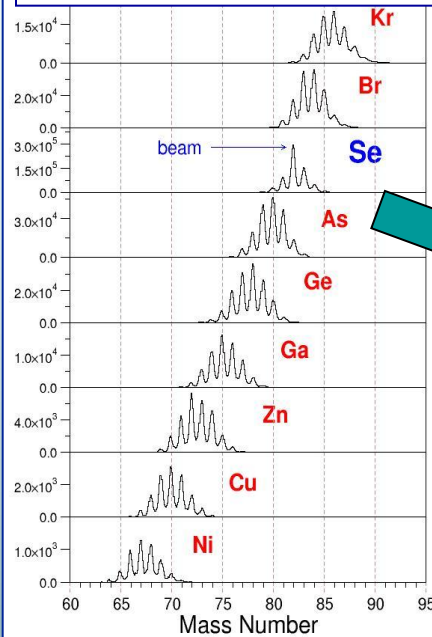


J.R. Brown et al.,
Phys. Rev. C 80, 011306(R) (2009)

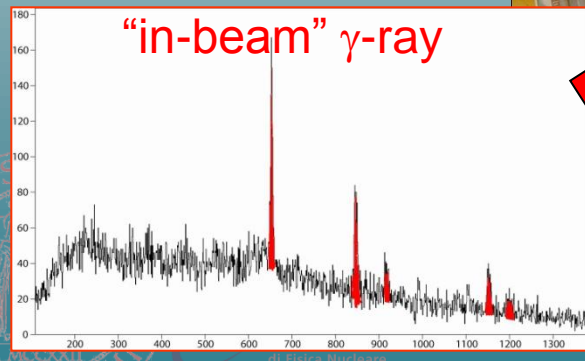
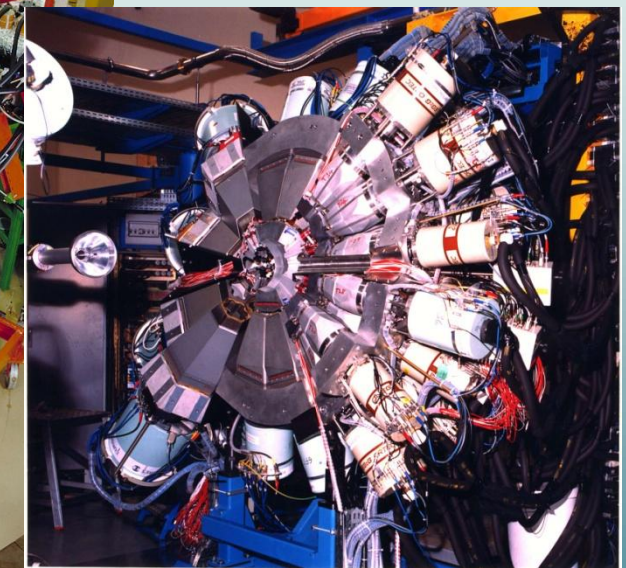
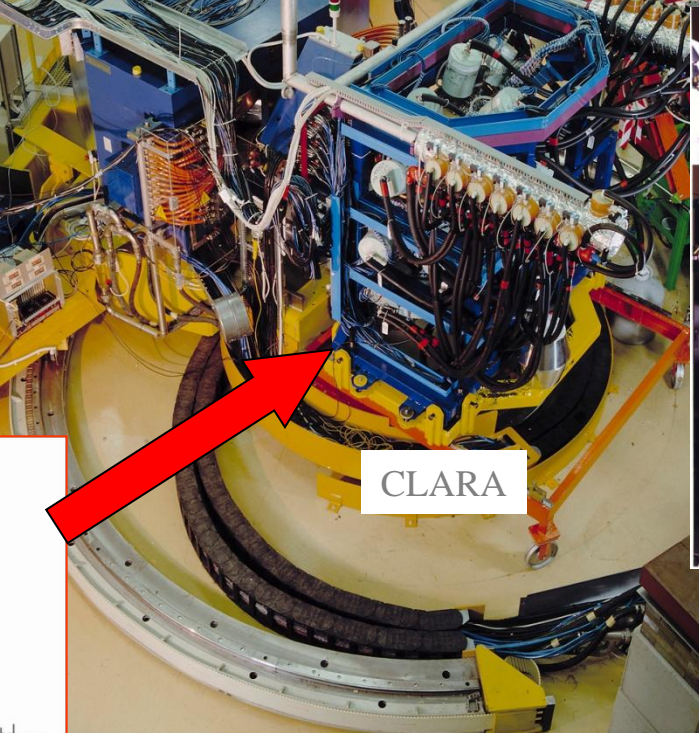


Mirror nuclei with multinucleon transfer

A & Z identification

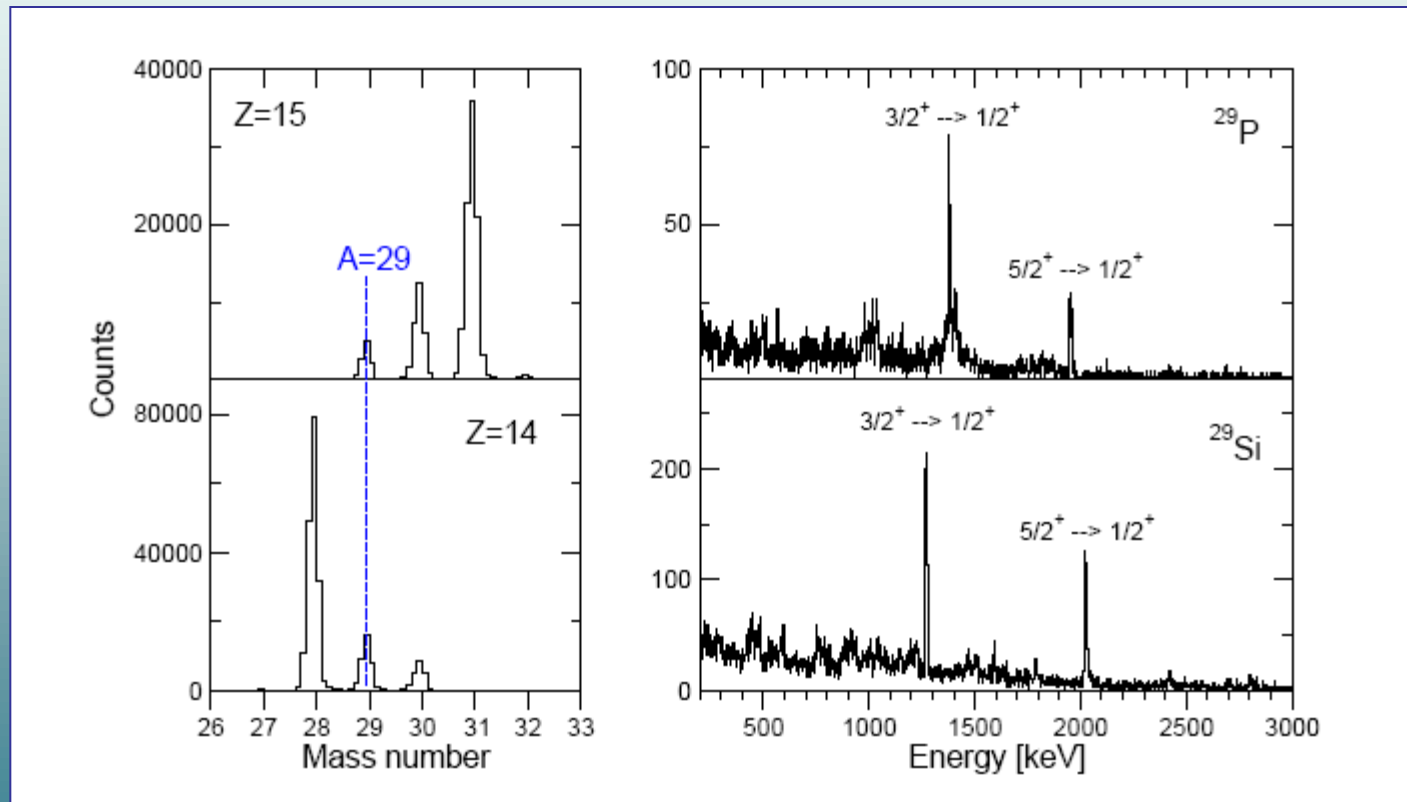
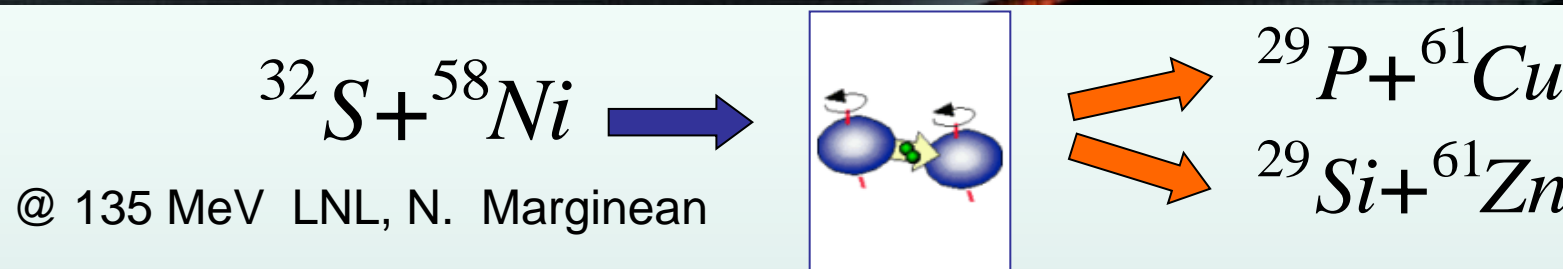


Prisma + CLARA
@LNL, Italy



Efficiency $\sim 3\%$
Peak/Total $\sim 50\%$
FWHM ~ 10 keV @ $v/c = 10\%$

Mirror nuclei with multinucleon transfer



PRISMA

CLARA

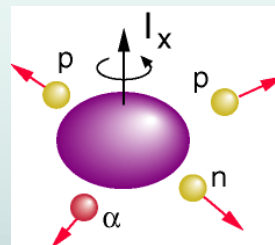


INFN

Istituto Nazionale
di Fisica Nucleare

3. Measuring the evaporated particles

With this method we do not measure directly the final residue but the particles emitted from the compound nucleus



charged particles

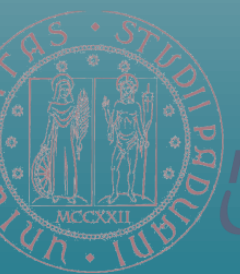
neutrons

We need detectors
with high efficiency



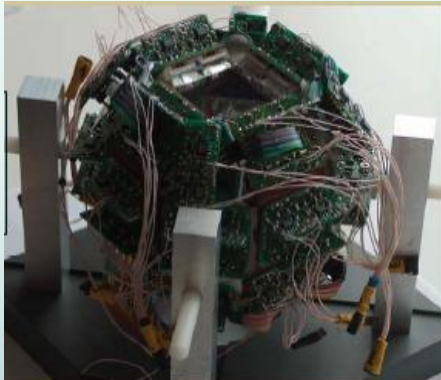
Advantage: more flexible than recoil mass spectrometry
→ more channels can be measured!

Disadvantage: not as clean as RMS
If neutrons are needed, it may be much less efficient



Charged-particle detectors

DIAMANT



86 CsI(Tl) elements scintillators

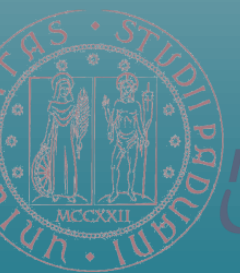
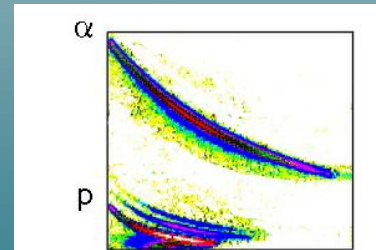
efficiency: protons ~70%
alphas ~ 50%

EUCLIDES



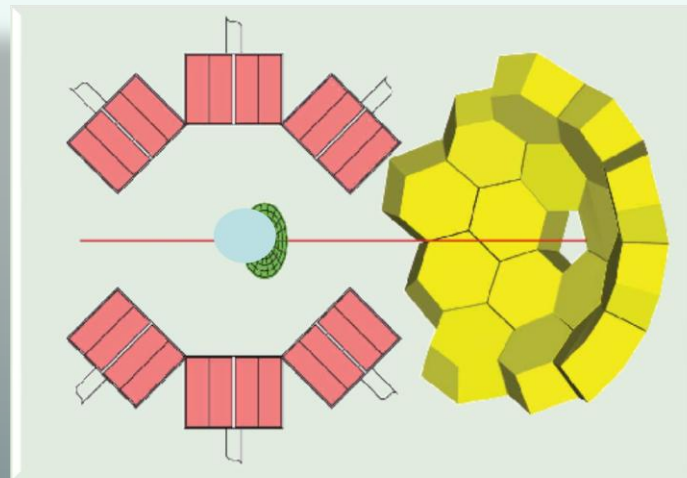
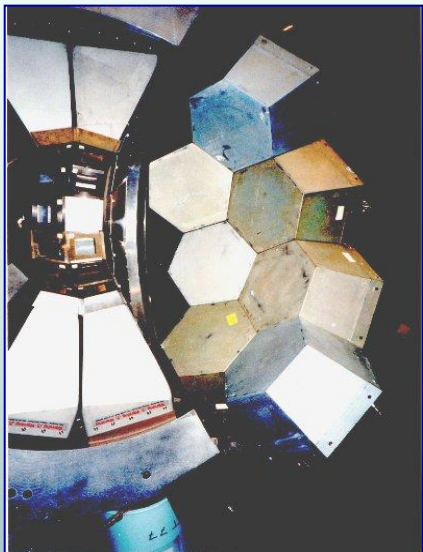
Si E- Δ E telescopes

efficiency: protons ~70%
alphas ~ 40%

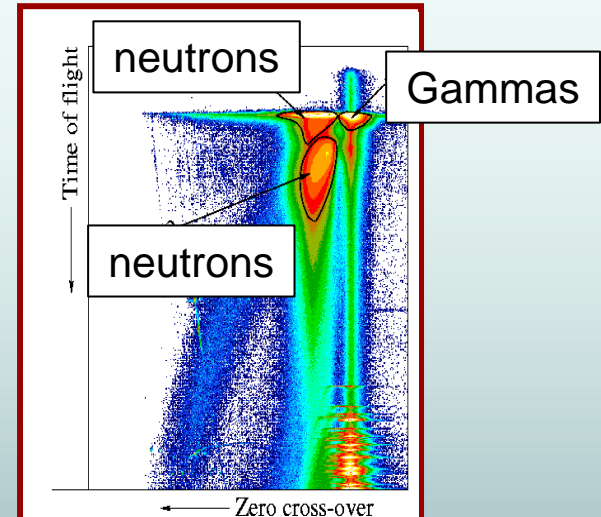


INFN
Istituto Nazionale
di Fisica Nucleare

Neutron detection systems



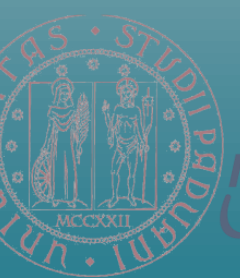
EXOGAM + N-Wall @ GANIL



Detectors placed downstream of the target position

Large volume liquid scintillators coupled to photo-multipliers tubes.
Usually replace some of the forward-most Ge detectors of the array

Efficiency ~ 25%

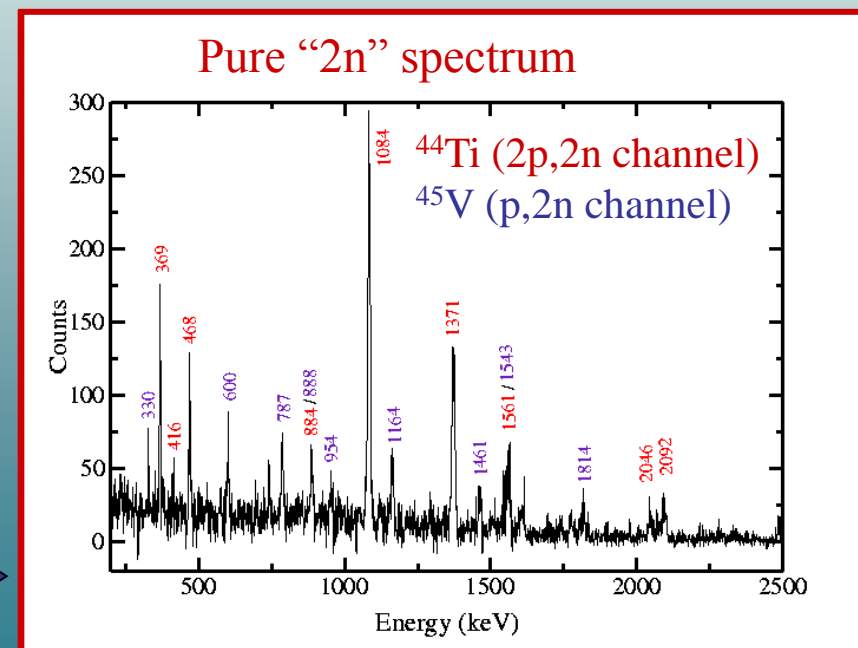
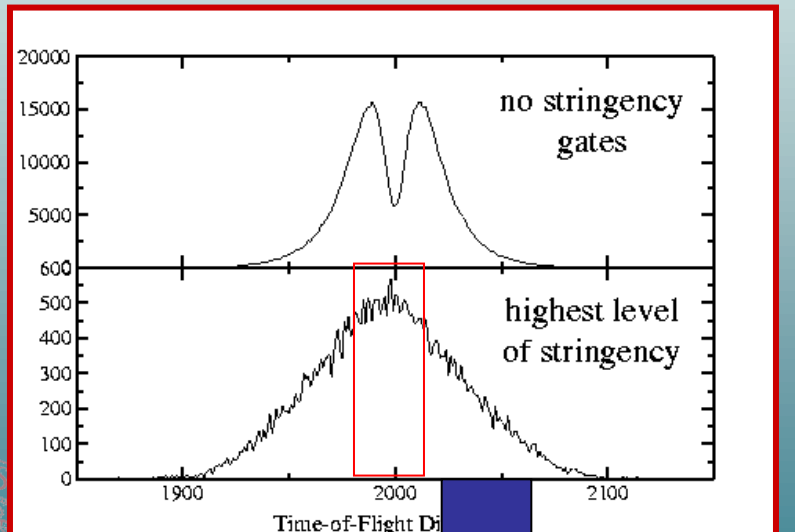
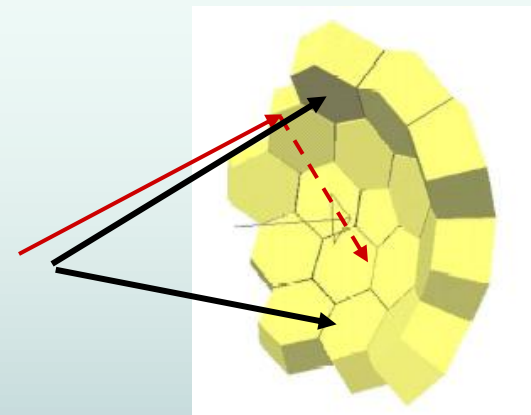


Discrimination using time-of-flight data

Problem: one neutron scattered between two detectors looks like two neutrons...

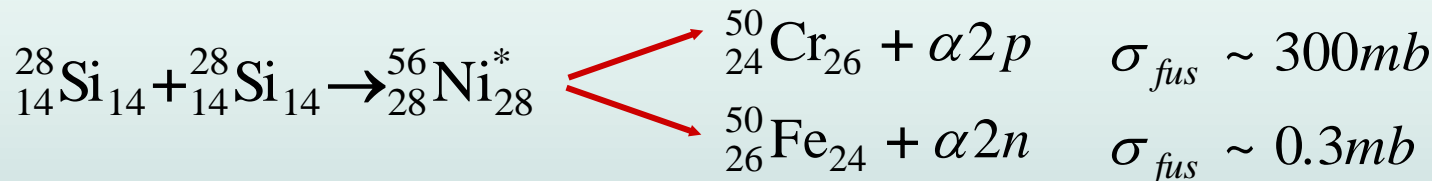
A single scattered neutron → different times-of-flight recorded

Genuine 2-neutron event → similar time-of-flight recorded



An example: production of ^{50}Fe

Experiment for ^{50}Fe , LNL



EUROBALL: High efficiency ($e_{ph} \sim 8\%$) and high granularity (209 crystals) HpGe array.

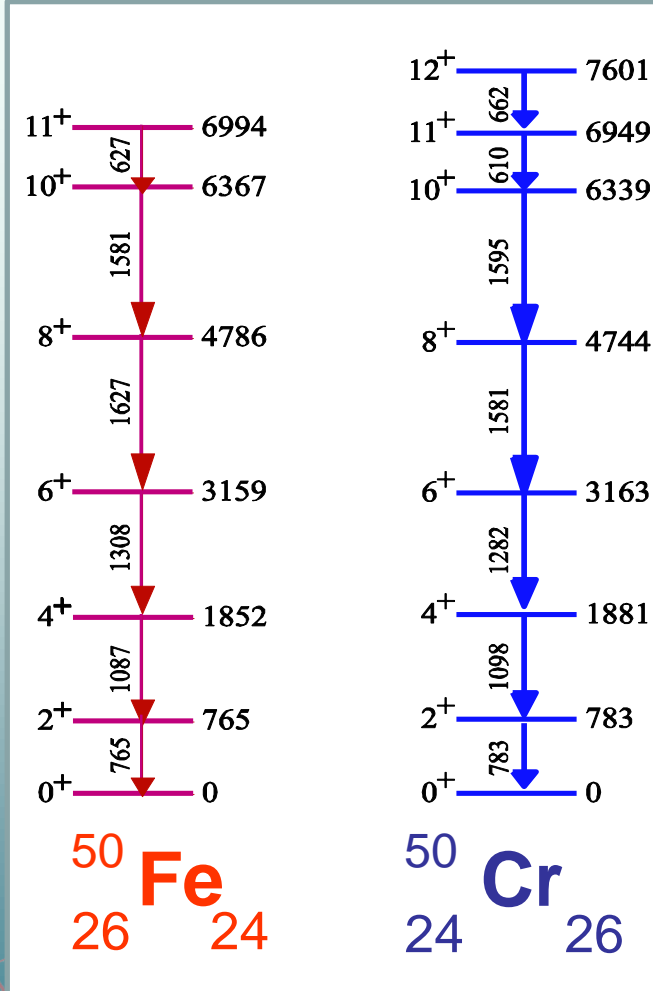
26 Clover detectors ($\times 4$ crystals) & 15 Clusters ($\times 7$ crystals).

ISIS: Charged-particle detector array - 40 Si E-DE telescopes, total efficiency $e_p \sim 70\%$, $e_a \sim 40\%$

NEUTRON WALL: 50 detector elements - BC501A Liquid Scintillator. Efficiency (reaction dependent) $e_{1n} \sim 25\%$.

S.M. Lenzi et al., Phys. Rev. Lett 87 (2001) 122501

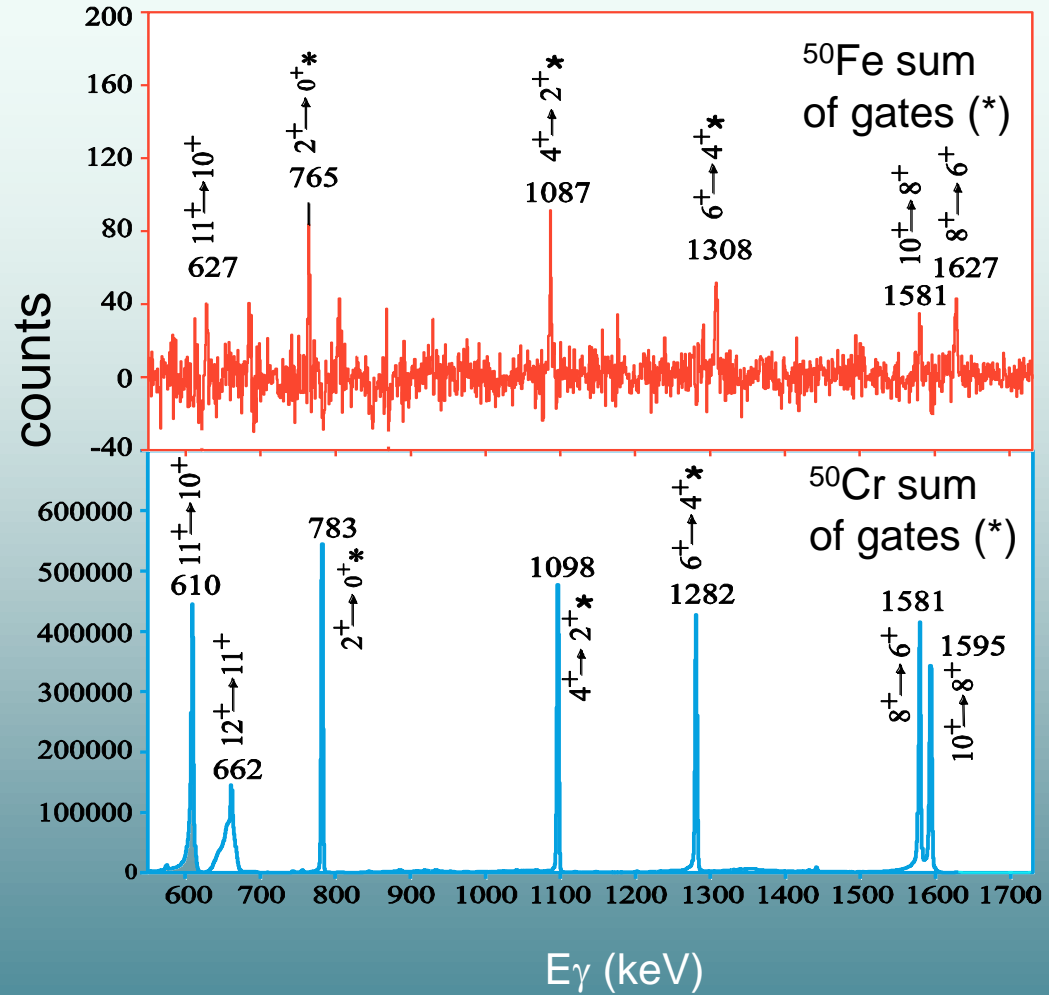
First observation of excited states in ^{50}Fe



$$\sigma(\text{Fe})/\sigma(\text{Cr}) \approx 10^{-4}$$

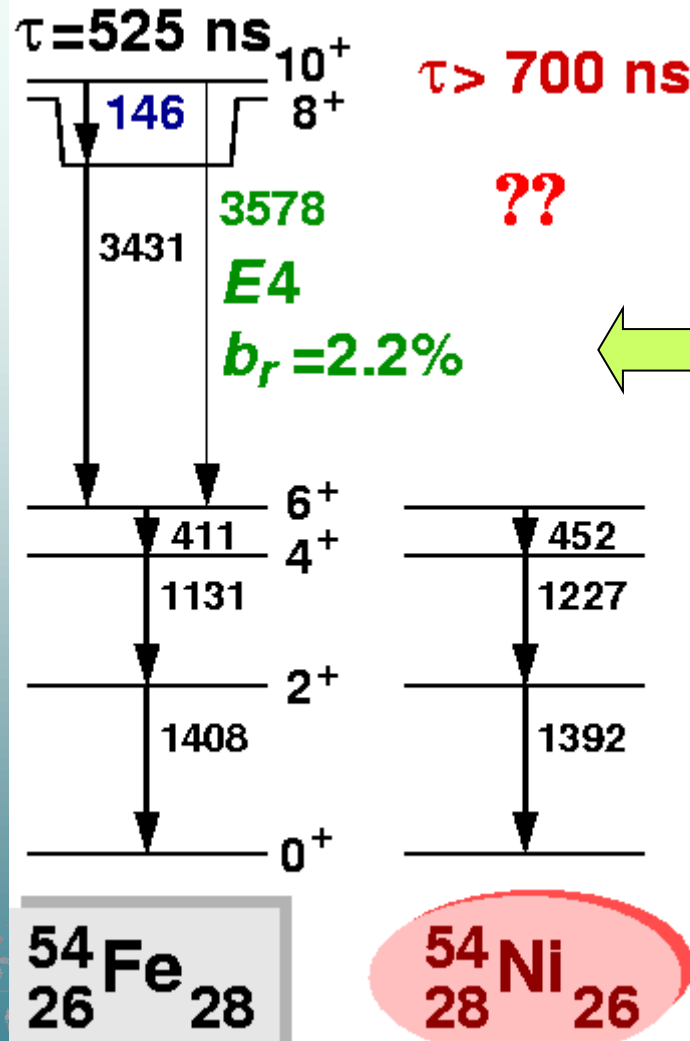


Istituto Nazionale
di Fisica Nucleare

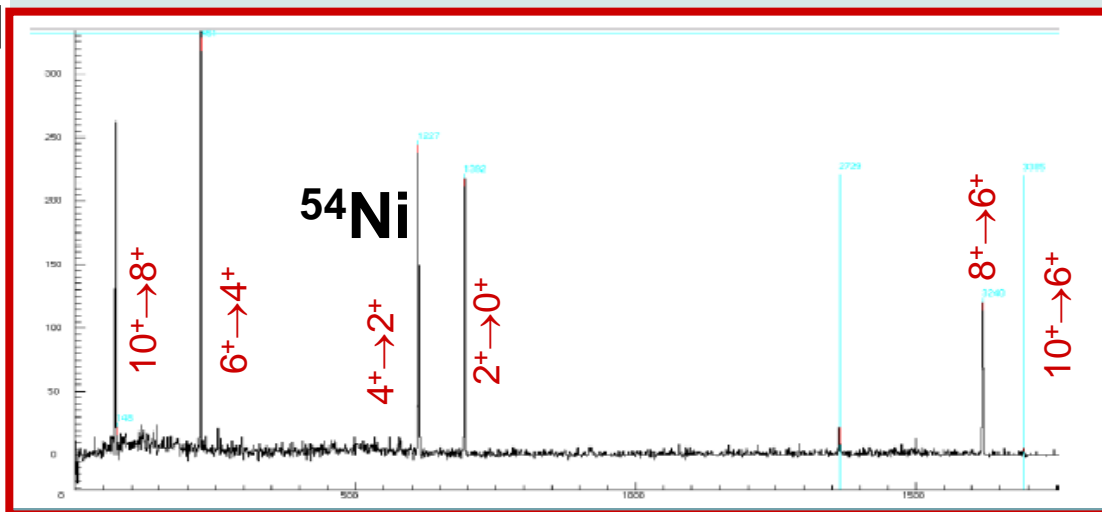


SML et al., Phys. Rev. Lett. 87, 122501 (2001)

Spectroscopy with exotic stopped beams

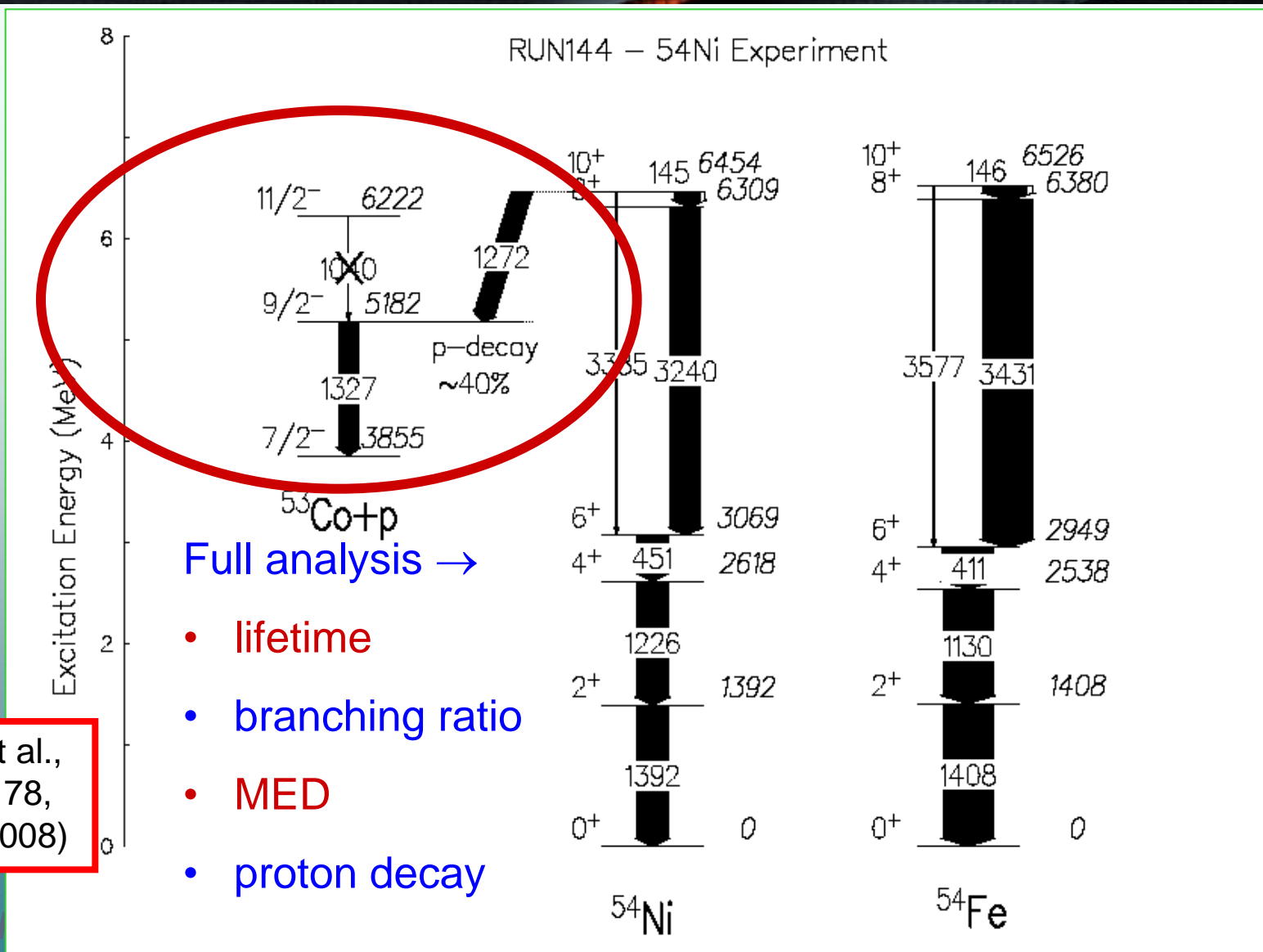


Fragmentation of ^{58}Ni beam
Secondary beam of ^{54}Ni in the
isomeric state 10^+



States in ^{54}Ni known up to the 6^+ ,
A.Gadea et al. Phys. Rev. Lett. 97 (2006)
152501 (EB+EUCLIDES+N-Wall)

Gamma and proton decay of ^{54}Ni



3. Theoretical tools for CED

First part

Basic Shell Model

The hamiltonian (only two-body forces)

$$H = \sum_{i=1}^A \frac{\vec{p}_i^2}{2m} + \frac{1}{2} \sum_{i,j=1}^A V_{ij}(\vec{r})$$

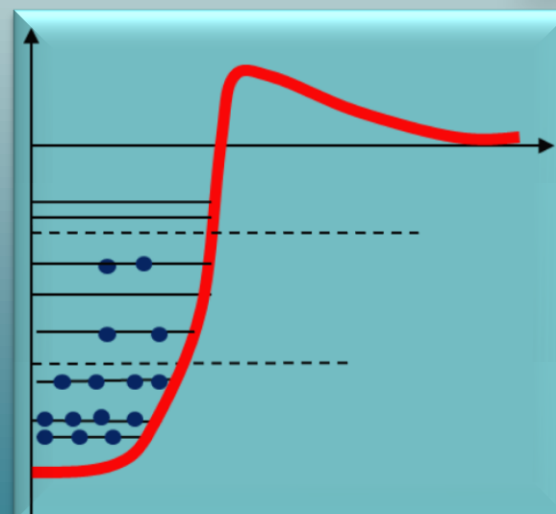
$$H = \sum_{i=1}^A \left(\frac{\vec{p}_i^2}{2m} + U(r_i) \right) + \sum_{i,j=1}^A V_{ij}(|\vec{r}_i - \vec{r}_j|) - \sum_{i=1}^A U(r_i) = H_0 + H_{res}$$

$$H_0 \phi(\mathbf{r}_1, \dots, \mathbf{r}_A) = E_0 \phi(\mathbf{r}_1, \dots, \mathbf{r}_A)$$

$$E_0 = \sum_i \varepsilon_i^{(0)}$$

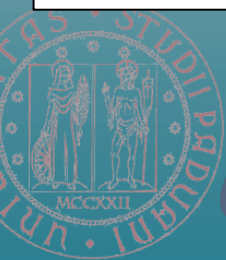
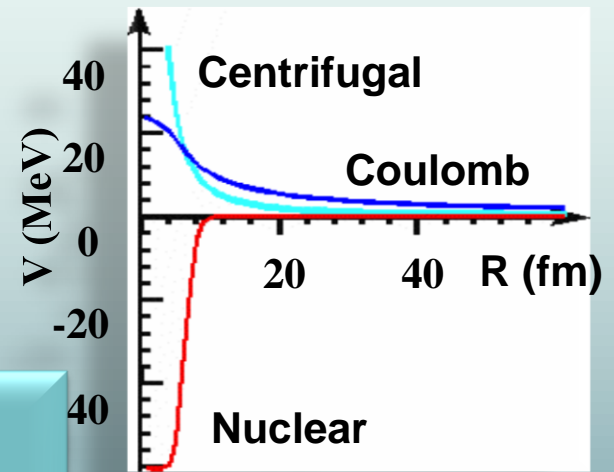
Configuration

$$\phi = \frac{1}{\sqrt{A!}} \det \begin{pmatrix} \psi_1(r_1) & \cdots & \psi_1(r_A) \\ \vdots & \ddots & \vdots \\ \psi_A(r_1) & \cdots & \psi_A(r_A) \end{pmatrix}$$



spherical mean field

$U(r)$ is a central (1-body) potential

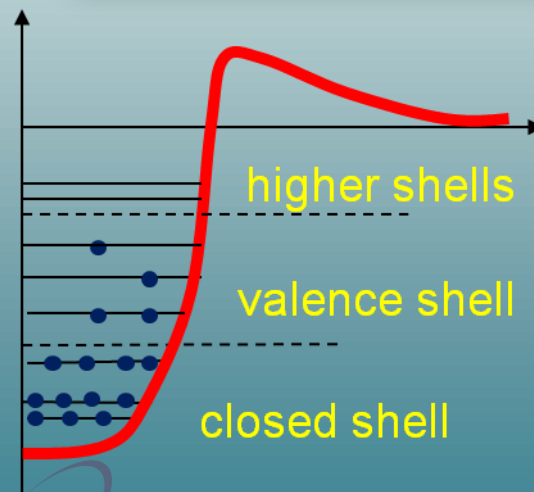


Configuration mixing

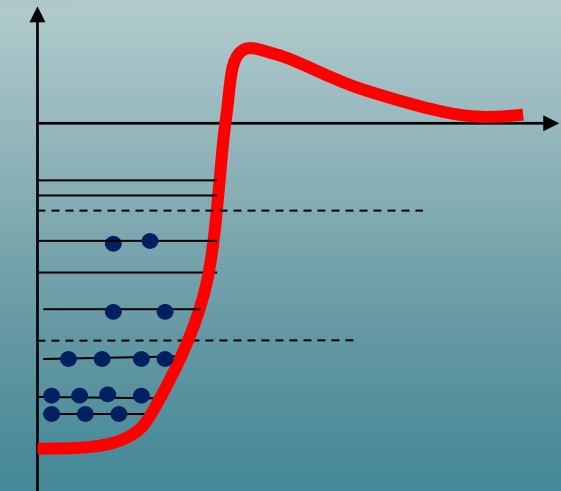
$$\phi = \frac{1}{\sqrt{A!}} \det \begin{pmatrix} \psi_1(r_1) & \dots & \psi_1(r_A) \\ \vdots & \ddots & \vdots \\ \psi_A(r_1) & \dots & \psi_A(r_A) \end{pmatrix}$$

$$\mathcal{H} = \begin{pmatrix} \langle \phi_1 | H | \phi_1 \rangle & \langle \phi_1 | H | \phi_2 \rangle & \dots \\ \langle \phi_2 | H | \phi_1 \rangle & \langle \phi_2 | H | \phi_2 \rangle & \dots \\ \langle \phi_3 | H | \phi_1 \rangle & & \vdots \end{pmatrix} = \begin{pmatrix} E_1 \\ & E_2 \\ & & \ddots \end{pmatrix}$$

$$\Psi = \sum_i^{\infty} c_i \phi_i$$



Mixing of configurations
due to the residual interaction



Effective Hamiltonian

We limit the space to a reduced set of shells.
The Hamiltonian becomes **an effective hamiltonian** H_{eff} that accounts for the missing space.

$$H_{\text{eff}} = H_m + H_M$$

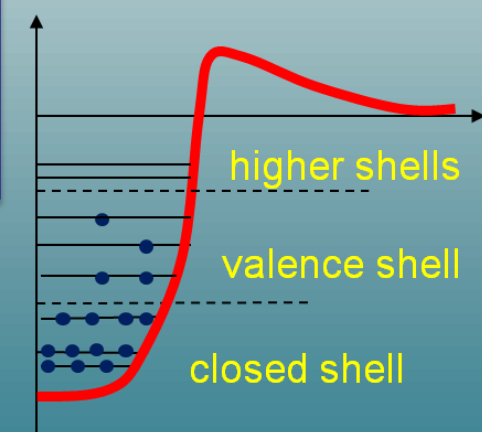
monopole Multipole

$$H_m$$

- “unperturbed” energy of the different configurations in which the valence nucleons are distributed
- determines the single particle energies
- dominant role far from stability

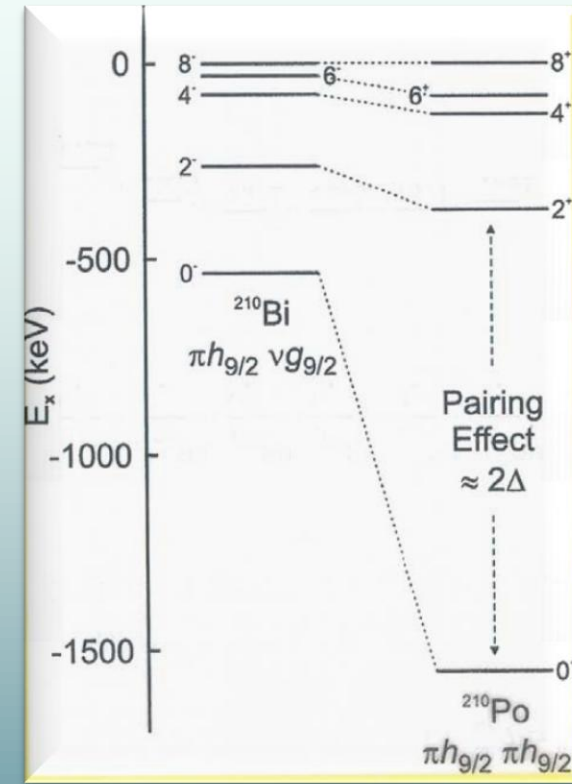
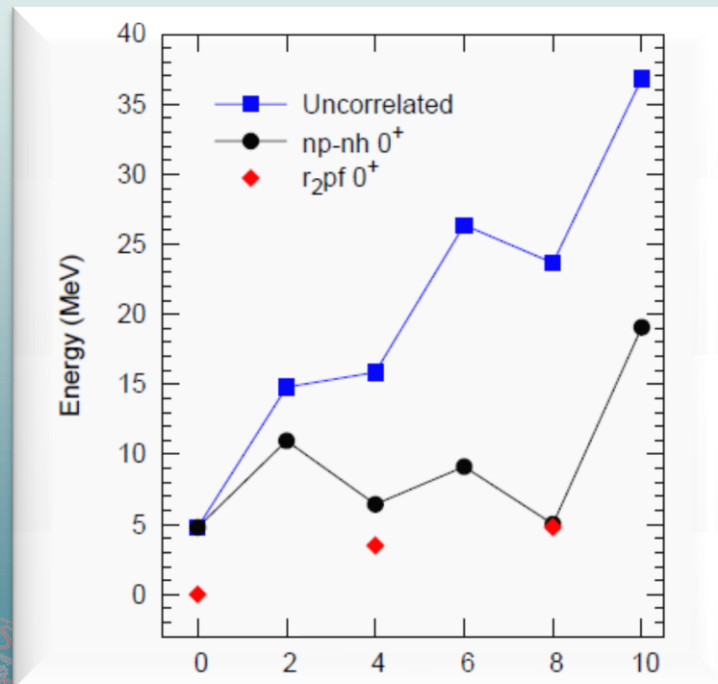
$$H_M$$

- correlations
- mixing of configurations
- coherence
- energy gains



Effect of the correlations

The multipole Hamiltonian H_M is dominated by the pairing and the quadrupole-quadrupole forces



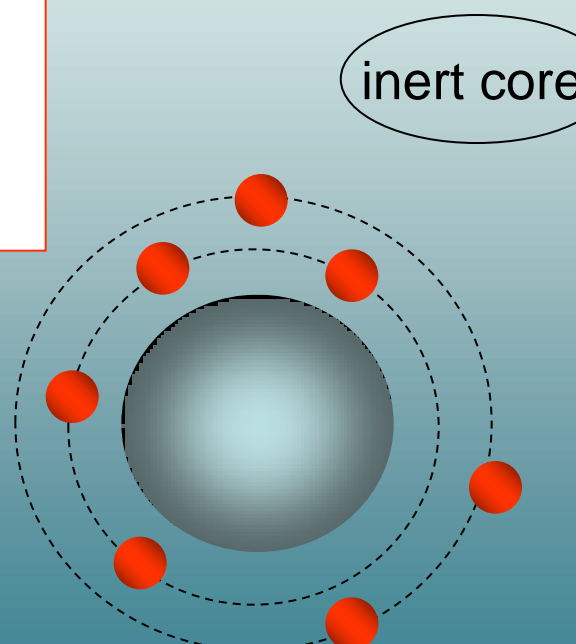
The fact that some nuclei display collective behaviour depends on the structure of the spherical field near the Fermi surface for both protons and neutrons

Ingredients for the Shell Model calculations

- 1) an inert core
- 2) a valence space
- 3) an effective interaction that mocks up the general hamiltonian in the restricted basis

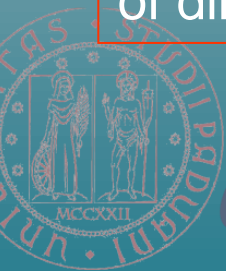
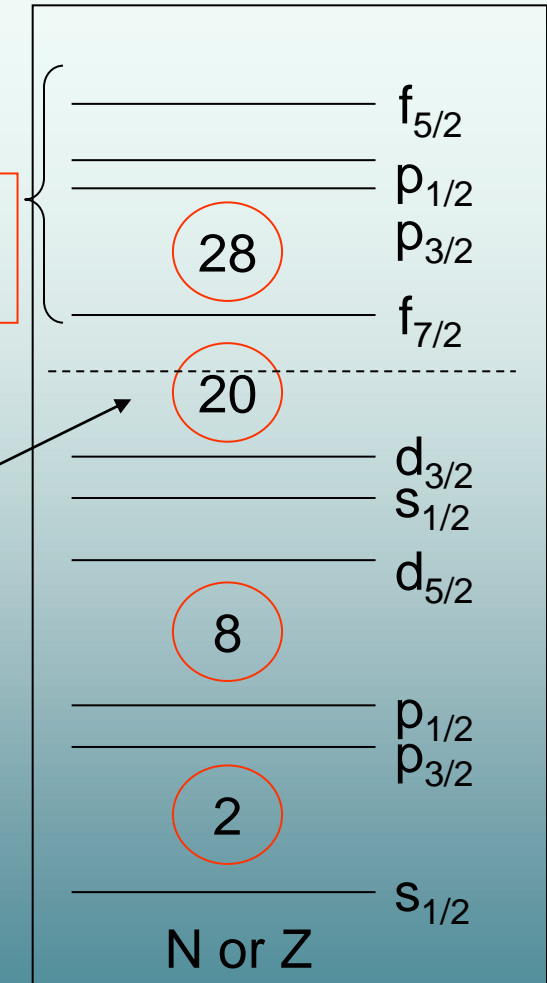
The choice is determined by the limits in computing time and memory: large dimension of the matrices to be diagonalised.

Current codes diagonalize matrices of dimension $\sim 10^{10}$



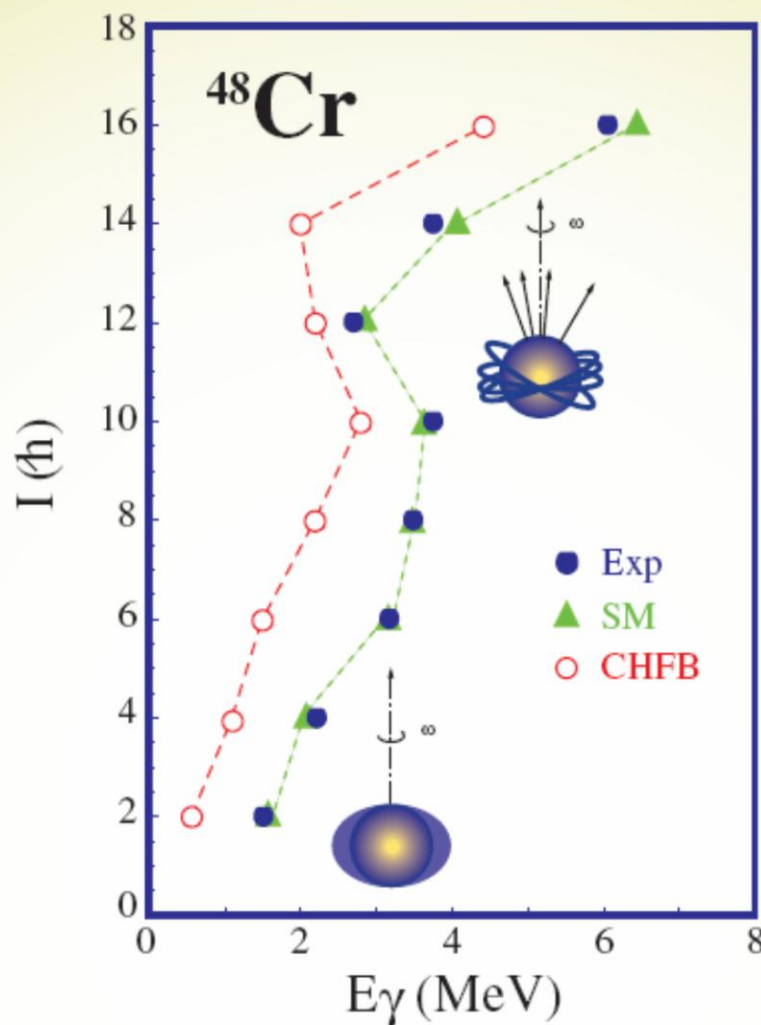
the valence space

inert core

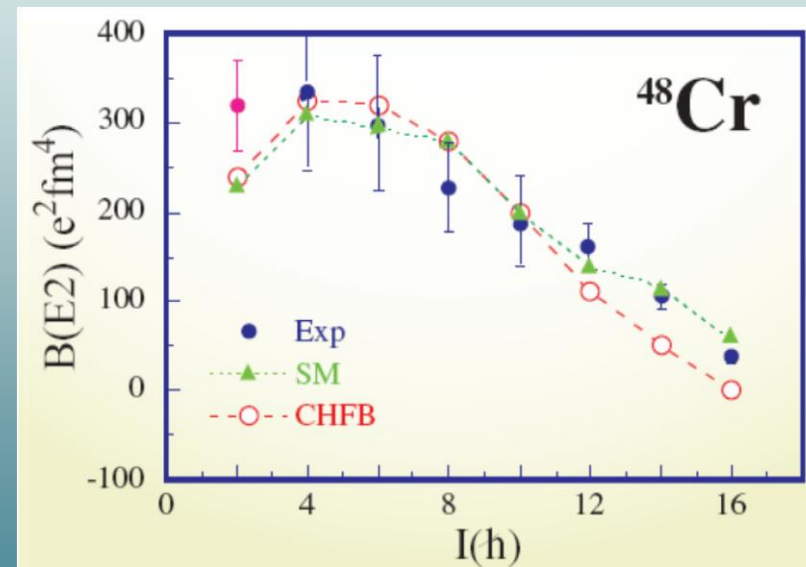


Istituto Nazionale
di Fisica Nucleare

Shell model and collective phenomena



Shell model calculations in the full fp shell give an excellent description of the structure of collective rotations in nuclei of the $f_{7/2}$ shell



Theory: E. Caurier et al., Phys.Rev.Lett. 75(1995)225

Experiments: S. M. Lenzi et al., Z.Phys.A354(1996)117 - F. Brandolini et al., Nucl.Phys.A642(1998)387



di Fisica Nucleare

Lecture 2

The end